Transverse Spin Structure of the Nucleon from Lattice-QCD Simulations

M. Göckeler,[1] Ph. Hägler,[2,*] R. Horsley,[3] Y. Nakamura,[4] D. Pleiter,[4] P. E. L. Rakow,[5] A. Schäfer,[1] G. Schierholz,[6,4] H. Stüben,[7] and J. M. Zanotti[3]

(QCDSF and UKQCD Collaborations)

[1]*Institut für Theoretische Physik, Universität Regensburg, 93040 Regensburg, Germany*
[2]*Physik-Department der TU München, Institut für Theoretische Physik T39, James-Franck-Straße, 85747 Garching, Germany*
[3]*School of Physics, University of Edinburgh, Edinburgh EH9 3JZ, United Kingdom*
[4]*John von Neumann-Institut für Computing NIC/DESY, 15738 Zeuthen, Germany*
[5]*Theoretical Physics Division, Department of Mathematical Sciences, University of Liverpool, Liverpool L69 3BX, United Kingdom*
[6]*Deutsches Elektron-Synchrotron DESY, 22603 Hamburg, Germany*
[7]*Konrad-Zuse-Zentrum für Informationstechnik Berlin, 14195 Berlin, Germany*
(Received 9 January 2007; published 29 May 2007)

We present the first calculation in lattice QCD of the lowest two moments of transverse spin densities of quarks in the nucleon. They encode correlations between quark spin and orbital angular momentum. Our dynamical simulations are based on two flavors of clover-improved Wilson fermions and Wilson gluons. We find significant contributions from certain quark helicity flip generalized parton distributions, leading to strongly distorted densities of transversely polarized quarks in the nucleon. In particular, based on our results and recent arguments by Burkardt [Phys. Rev. D **72**, 094020 (2005)], we predict that the Boer-Mulders function $h_1^\perp$, describing correlations of transverse quark spin and intrinsic transverse momentum of quarks, is large and negative for both up and down quarks.

DOI: 10.1103/PhysRevLett.98.222001 PACS numbers: 12.38.Gc, 14.20.Dh

Introduction.—The transverse spin (transversity) structure of the nucleon received a lot of attention in recent years from both theory and experiment as it provides a new perspective on hadron structure and QCD evolution (for a review, see [1]). A central object of interest is the quark transversity distribution $\delta q(x) = h_1(x)$, which describes the probability of finding a transversely polarized quark with longitudinal momentum fraction x in a transversely polarized nucleon [2]. Much progress has been made in the understanding of so-called transverse momentum dependent parton distribution functions (TMD PDFs) like, e.g., the Sivers function $f_{1T}^\perp(x, k_\perp^2)$ [3], which measures the correlation of the intrinsic quark transverse momentum $k_\perp$ and the transverse nucleon spin $S_\perp$, as well as the Boer-Mulders function $h_1^\perp(x, k_\perp^2)$ [4], describing the correlation of $k_\perp$ and the transverse quark spin $s_\perp$. While the Sivers function is beginning to be understood, still very little is known about the sign and size of the Boer-Mulders function.

A particularly promising approach is based on 3-dimensional densities of quarks in the nucleon, $\rho(x, b_\perp, s_\perp, S_\perp)$ [5], representing the probability of finding a quark with momentum fraction x and transverse spin $s_\perp$ at distance $b_\perp$ from the center of momentum of the nucleon with transverse spin $S_\perp$. As we will see below, these transverse spin densities show intriguing correlations of transverse coordinate and spin degrees of freedom. According to Burkardt [6,7], they are directly related to the above mentioned Sivers and Boer-Mulders functions. Our lattice results on transverse spin densities therefore provide for the first time quantitative predictions for the signs and sizes of these TMD PDFs and the corresponding experimentally accessible asymmetries.

Lattice calculations give access to x moments of transverse quark spin densities [5]

$$\begin{aligned}\rho^n &= \int_{-1}^{1} dx x^{n-1} \rho(x, b_\perp, s_\perp, S_\perp)\\ &= \frac{1}{2}\Big\{A_{n0}(b_\perp^2) + s_\perp^i S_\perp^i\Big(A_{Tn0}(b_\perp^2) - \frac{\Delta_{b_\perp}\tilde{A}_{Tn0}(b_\perp^2)}{4m^2}\Big)\\ &\quad + \frac{b_\perp^j \epsilon^{ji}}{m}[S_\perp^i B'_{n0}(b_\perp^2) + s_\perp^i \overline{B}'_{Tn0}(b_\perp^2)]\\ &\quad + s_\perp^i(2b_\perp^i b_\perp^j - b_\perp^2\delta^{ij})S_\perp^j \frac{1}{m^2}\tilde{A}''_{Tn0}(b_\perp^2)\Big\},\end{aligned} \tag{1}$$

where $\rho^n = \rho^n(b_\perp, s_\perp, S_\perp)$ and m is the nucleon mass. The $b_\perp$-dependent nucleon generalized form factors (GFFs) $A_{n0}(b_\perp^2), A_{Tn0}(b_\perp^2), \ldots$ in Eq. (1) are related to GFFs in momentum space $A_{n0}(t), A_{Tn0}(t), \ldots$ by a Fourier transformation

$$f(b_\perp^2) \equiv \int \frac{d^2\Delta_\perp}{(2\pi)^2} e^{-ib_\perp\cdot\Delta_\perp} f(t = -\Delta_\perp^2), \tag{2}$$

where $\Delta_\perp$ is the transverse momentum transfer to the nucleon. Their derivatives are defined by $f' \equiv \partial_{b_\perp^2} f$ and $\Delta_{b_\perp} f \equiv 4\partial_{b_\perp^2}(b_\perp^2 \partial_{b_\perp^2})f$. The generalized form factors in this work are directly related to x moments of the corresponding vector and tensor generalized parton distributions (GPDs) (for a review, see [8]). The probability interpretation of GPDs in impact parameter space was first noted in [9]. Apart from the orbitally symmetric monopole terms in the second line of Eq. (1), there are two dipole structures present in the third line of Eq. (1), $b^j_\perp \epsilon^{ji} s^i_\perp$ and $b^j_\perp \epsilon^{ji} S^i_\perp$. The fourth line in Eq. (1) corresponds to a quadrupole term. The (derivatives of the) three GFFs $B_{n0}(b_\perp)$, $\bar{B}_{Tn0}(b_\perp)$, and $\tilde{A}_{Tn0}(b_\perp)$ thus determine how strongly the orbital symmetry in the transverse plane is distorted by the dipole and the quadrupole terms.

The GFFs $A_{n0}(t), A_{Tn0}(t), \ldots$ parametrize off-forward nucleon matrix elements of certain local quark operators. For the lowest moment $n = 1$ one finds $A_{10}(t) = F_1(t)$, $B_{10}(t) = F_2(t)$, and $A_{T10}(t) = g_T(t)$ where F_1, F_2, and g_T are the Dirac, Pauli, and tensor nucleon form factors, respectively. A concrete example of the corresponding parametrization for $n = 1$ is given by [10,11]

$$\langle P'\Lambda'|\mathcal{O}_T^{\mu\nu}|P\Lambda\rangle = \bar{u}(P',\Lambda')\Big\{\sigma^{\mu\nu}\gamma_5\Big(A_{T10}(t) - \frac{t}{2m^2}\tilde{A}_{T10}(t)\Big) + \frac{\epsilon^{\mu\nu\alpha\beta}\Delta_\alpha\gamma_\beta}{2m}\bar{B}_{T10}(t) - \frac{\Delta^{[\mu}\sigma^{\nu]\alpha}\gamma_5\Delta_\alpha}{2m^2}\tilde{A}_{T10}(t)\Big\}u(P,\Lambda), \quad (3)$$

where $\mathcal{O}_T^{\mu\nu} = \bar{q}\sigma^{\mu\nu}\gamma_5 q$ is the lowest element of the tower of local leading twist tensor (quark helicity flip) operators. Parametrizations for higher moments $n \geq 1$ in terms of tensor GFFs and their relation to GPDs are given in [11]. As it is very challenging to access tensor GPDs in experiment [12], input from lattice-QCD calculations is crucial in this case.

Simulation results.—Our lattice calculations are based on configurations generated with $n_f = 2$ dynamical nonperturbatively $\mathcal{O}(a)$ improved Wilson fermions and Wilson gluons. Simulations have been performed at four different couplings $\beta = 5.20, 5.25, 5.29, 5.40$ with up to five different $\kappa = \kappa_{\rm sea}$ values per β, on lattices of $V \times T = 16^3 \times 32$ and $24^3 \times 48$. The lattice spacings are below 0.1 fm, the range of pion masses extends down to 400 MeV, and the spatial volumes are as large as $(2.1\ \mathrm{fm})^3$. The lattice scale a in physical units has been set using a Sommer scale of $r_0 = 0.467$ fm [13,14]. The computationally demanding disconnected contributions are not included. We expect, however, that they are small for the tensor GFFs [15]. We use nonperturbative renormalization [16] to transform the lattice results to the modified minimal subtraction ($\overline{\rm MS}$) scheme at a scale of 4 GeV^2. The calculation of GFFs in lattice QCD follows standard methods (see, e.g., [17–19]).

In Fig. 1, we show as an example results for the GFFs $\bar{B}^{u,d}_{T(n=1,2)0}(t)$, corresponding to the lowest two moments $n = 1, 2$ of the GPD $\bar{E}^{u,d}_T(x,\xi,t)$ [20], as a function of the momentum transfer squared t, for a pion mass of $m_\pi \approx 600$ MeV, a lattice spacing of $a \approx 0.08$ fm, and a volume of $V \approx (2\ \mathrm{fm})^3$. For the extrapolation to the forward limit ($t = 0$) and in order to get a functional parametrization of the lattice results, we fit all GFFs using a p-pole ansatz $F(t) = F_0/[1 - t/(pm_p^2)]^p$ with the three parameters $F_0 = F(t = 0)$, m_p, and p for each GFF. We consider this ansatz [21] to be more physical than previous ones as the rms radius $\langle r^2\rangle^{1/2} \propto m_p^{-1}$ is independent of p. It turns out that in most cases the statistics is not sufficient to determine all three parameters from a single fit to the lattice data. For a given generalized form factor, we therefore fix the power p first, guided by fits to selected data sets, and subsequently determine the forward value F_0 and the p-pole mass m_p by a full fit to the lattice data. Some GFFs show a quark flavor dependence of the value of p, which has already been observed in [22] for the Dirac form factor. For the examples in Fig. 1, we find for u quarks $\bar{B}^u_{T10}(t = 0) = 3.34(8)$ with $m_p = 0.907(75)$ GeV, $\bar{B}^u_{T20}(t = 0) = 0.750(32)$ with $m_p = 1.261(40)$ GeV, and for d quarks $\bar{B}^d_{T10}(t = 0) = 2.06(6)$ with $m_p = 0.889(48)$ GeV, $\bar{B}^d_{T20}(t = 0) = 0.473(22)$ with $m_p = 1.233(27)$ GeV (all for $p = 2.5$). We have checked that the final p-pole parametrizations only show a mild dependence on the value of p chosen prior to the fit. In order to see to what extent our calculation is affected by discretization errors, we plot as an example in Fig. 2 the tensor charge $A_{T10}(t = 0) = g_T(t = 0)$ versus the lattice spacing squared, for a fixed $m_\pi \approx 600$ MeV. The discretization errors seem to be smaller than the statistical errors, and we will neglect any dependence of the GFFs on a in the following. Taking our investigations of the volume dependence of the nucleon mass and the axial vector form factor g_A [13,23] as a guide, we estimate that the finite volume

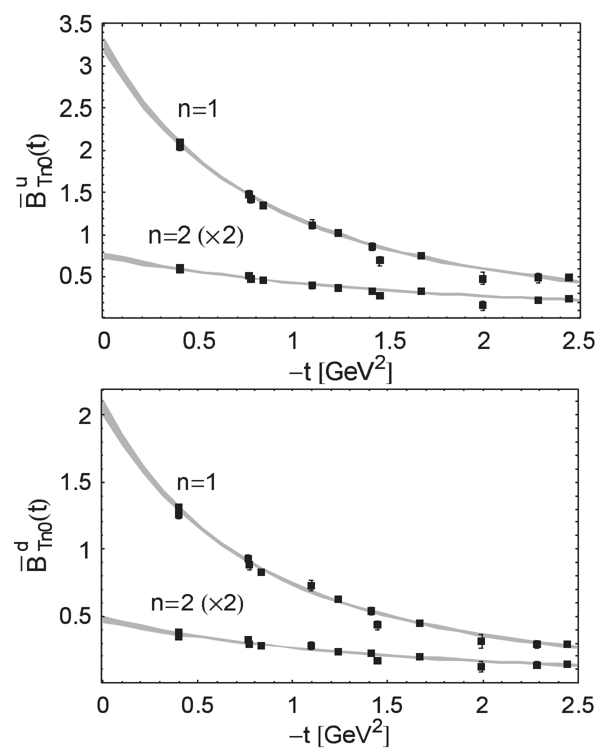

FIG. 1. Results for the generalized form factors $\bar{B}_{T(n=1,2)0}(t)$. The corresponding p-pole parametrizations are shown by the shaded error bands.

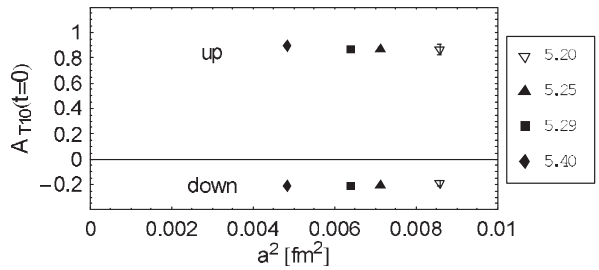

FIG. 2. Study of discretization errors of the tensor charge $A_{T10}(t=0) = g_T(t=0)$ for up and down quarks at a pion mass of $m_\pi \approx 600$ MeV.

effects for the lattices and observables studied in this work are small and may be neglected.

As an example of the pion mass dependence of our results, we show in Fig. 3 the GFFs $\bar{B}^u_{T(n=1,2)0}(t=0)$ versus m_π^2. Unfortunately we cannot expect chiral perturbation theory predictions [24] to be applicable to most of our lattice data points, for which the pion mass is still rather large. To get an estimate of the GFFs at the physical point, we extrapolate the forward moments and the p-pole masses using an ansatz linear in m_π^2. The results of the corresponding fits are shown as shaded error bands in Fig. 3. At $m_\pi^{\text{phys}} = 140$ MeV, we find $\bar{B}^u_{T10}(t=0) = 2.93(13)$, $\bar{B}^d_{T10}(t=0) = 1.90(9)$ and $\bar{B}^u_{T20}(t=0) = 0.420(31)$, $\bar{B}^d_{T20}(t=0) = 0.260(23)$. These comparatively large values already indicate a significant impact of this tensor GFF on the transverse spin structure of the nucleon, as will be discussed below. Since the (tensor) GPD $\bar{E}_T$ can be seen as the analogue of the (vector) GPD E, we may define an anomalous tensor magnetic moment [7], $\kappa_T \equiv \int dx \bar{E}_T(x,\xi,t=0) = \bar{B}_{T10}(t=0)$, similar to the standard anomalous magnetic moment $\kappa = \int dx E(x,\xi,t=0) = B_{10}(t=0) = F_2(t=0)$. While the u- and d-quark contributions to the anomalous magnetic moment are both large and of opposite sign, $\kappa^{\text{up}}_{\text{exp}} \approx 1.67$ and $\kappa^{\text{down}}_{\text{exp}} \approx -2.03$, we find large positive values for the anomalous tensor magnetic moment for both flavors, $\kappa^{\text{up}}_{T,\text{latt}} \approx 3.0$ and $\kappa^{\text{down}}_{T,\text{latt}} \approx 1.9$. Similarly large positive values have been obtained in a recent model calculation [25]. Large N_c considerations predict $\kappa^{\text{up}}_T \approx \kappa^{\text{down}}_T$ [26].

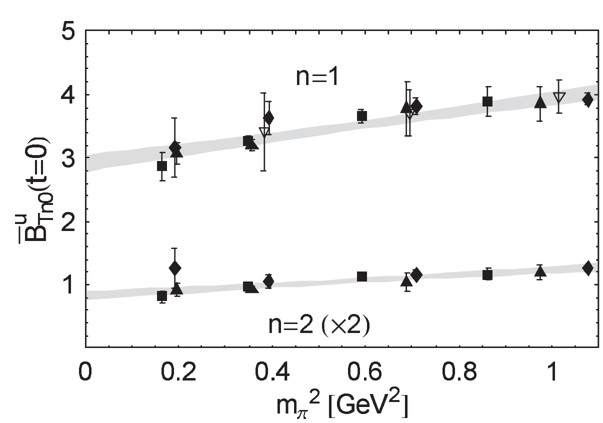

FIG. 3. Pion mass dependence of the generalized form factors $\bar{B}_{T(n=1,2)0}(t=0)$ for up quarks. The shaded error bands show extrapolations to the physical pion mass based on an ansatz linear in m_π^2. The symbols are as in Fig. 2.

Let us now discuss our results for $\rho^n(b_\perp, s_\perp, S_\perp)$ in Eq. (1). For the numerical evaluation we Fourier transform the p-pole parametrization to impact parameter ($b_\perp$) space. The parametrizations of the impact parameter dependent GFFs then depend only on the p-pole masses m_p and the forward values F_0. Before showing our final results, we would like to note that the moments of the transverse spin density can be written as the sum or difference of the corresponding moments for quarks and antiquarks, $\rho^n = \rho^n_q + (-1)^n \rho^n_{\bar{q}}$, because vector and tensor operators transform identically under charge conjugation. Although we expect contributions from antiquarks to be small in general, only the n-even moments must be strictly positive. In Fig. 4, we show the lowest moment $n = 1$ of spin densities for u and d quarks in the nucleon. Because of the large anomalous magnetic moments $\kappa^{u,d}$, we find strong distortions for unpolarized quarks in transversely polarized nucleons (left part of the figure). This has already been discussed in [6], and can serve as a dynamical explanation of the experimentally observed Sivers effect. Remarkably, we find even stronger distortions for transversely polarized quarks $s_\perp = (s_x, 0)$ in an unpolarized nucleon, as can be seen on the right-hand side of Fig. 4. The densities for u and for d quarks in this case are both deformed in positive b_y direction due to the large positive values for the tensor GFFs $\bar{B}^u_{T10}(t=0)$ and $\bar{B}^d_{T10}(t=0)$, in strong contrast to the distortions one finds for unpolarized quarks in a transversely polarized nucleon. All these observations are quite plausible if we assume that transverse quark spin and orbital angular momentum are aligned for u and d quarks. Based on this hypothesis, we expect that the densities for polarized quarks in an unpolarized (polarization-averaged) nucleon on the right-hand side of Fig. 4 are shifted in the same direction, e.g., upwards for quarks with spin in x direction in a nucleon moving towards the observer in z direction. The fact that the u-quark (d-quark) spin is predominantly oriented parallel (antiparallel) to the nucleon spin then implies that densities of unpolarized quarks in a polarized nucleon are shifted in opposite directions for u and d quarks, e.g., that the orbital motion of d quarks around the $(-x)$ direction leads to a larger d-quark density in the lower half-plane, as can be seen on the left-hand side of Fig. 4. It has been argued by Burkardt [7] that the deformed densities on the right-hand side of Fig. 4 are related to a nonvanishing Boer-Mulders function [4] $h_1^\perp$ which describes the correlation of intrinsic quark transverse momentum and the transverse quark spin $s_\perp$. According to [7] we have in particular $\kappa_T \sim -h_1^\perp$. If this conjecture is correct our results imply that the Boer-Mulders function is large and negative both for u and d quarks. The different strengths of transverse distortions found in the Sivers and Boer-Mulders cases indicate that

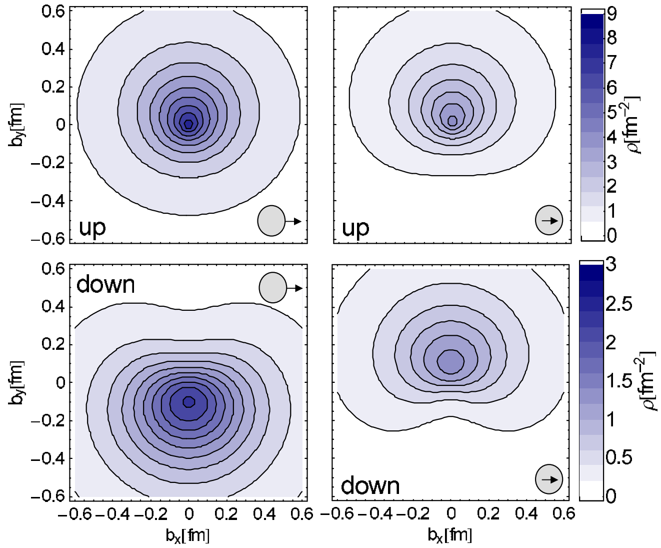

FIG. 4 (color online). Lowest moment ($n = 1$) of the densities of unpolarized quarks in a transversely polarized nucleon (left) and transversely polarized quarks in an unpolarized nucleon (right) for up (upper plots) and down (lower plots) quarks. The quark spins (inner arrows) and nucleon spins (outer arrows) are oriented in the transverse plane as indicated.

the latter correlation is stronger than the one between transverse quark and nucleon spin.

Figure 5 shows the $n = 2$ moment of the densities. Obviously, the pattern is very similar to that in Fig. 4, which supports our simple interpretation. The main difference is that the densities for the higher $n = 2$ moment are more peaked around the origin $b_\perp = 0$ as already observed in [27] for the vector and axial vector GFFs.

Conclusions.—We have presented first lattice results for the lowest two moments of transverse spin densities of quarks in the nucleon. Because of the large and positive contributions from the tensor GFF $\bar{B}_{Tn0}$ for up and for down quarks, we find strongly distorted spin densities for transversely polarized quarks in an unpolarized nucleon. According to Burkardt [7], this leads to the prediction of a sizable negative Boer-Mulders function [4] for up and down quarks, which may be confirmed in experiments at, e.g., Jefferson Lab and GSI Facility for Antiproton and Ion Research [28,29].

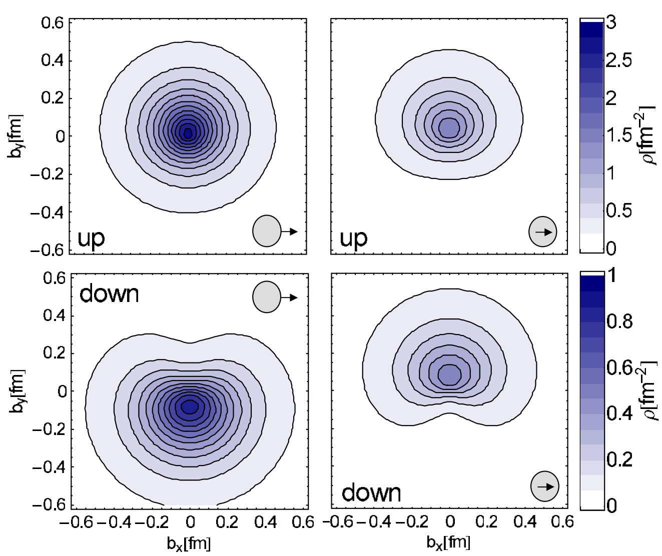

FIG. 5 (color online). Second moment ($n = 2$) of transverse spin densities. For details, see caption of Fig. 4.

The numerical calculations have been performed on the Hitachi No. SR8000 at LRZ (Munich), the apeNEXT at NIC/DESY (Zeuthen), and the BlueGene/L at NIC/FZJ (Jülich), EPCC (Edinburgh), and KEK (by the Kanazawa group as part of the DIK research programme). This work was supported by DFG (Forschergruppe Gitter-Hadronen-Phänomenologie and Emmy-Noether programme), HGF (Contract No. VH-NG-004), and EU I3HP (Contract No. RII3-CT-2004-506078).

*Electronic address: phaegler@ph.tum.de

[1] V. Barone, A. Drago, and P. G. Ratcliffe, Phys. Rep. **359**, 1 (2002).
[2] R. L. Jaffe and X. D. Ji, Phys. Rev. Lett. **67**, 552 (1991).
[3] D. W. Sivers, Phys. Rev. D **41**, 83 (1990).
[4] D. Boer and P. J. Mulders, Phys. Rev. D **57**, 5780 (1998).
[5] M. Diehl and Ph. Hägler, Eur. Phys. J. C **44**, 87 (2005).
[6] M. Burkardt, Nucl. Phys. **A735**, 185 (2004).
[7] M. Burkardt, Phys. Rev. D **72**, 094020 (2005).
[8] M. Diehl, Phys. Rep. **388**, 41 (2003).
[9] M. Burkardt, Phys. Rev. D **62**, 071503 (2000); **66**, 119903 (2002).
[10] M. Diehl, Eur. Phys. J. C **19**, 485 (2001).
[11] Ph. Hägler, Phys. Lett. B **594**, 164 (2004); Z. Chen and X. Ji, Phys. Rev. D **71**, 016003 (2005).
[12] J. C. Collins and M. Diehl, Phys. Rev. D **61**, 114015 (2000); D. Y. Ivanov *et al.*, Phys. Lett. B **550**, 65 (2002).
[13] A. Ali Khan *et al.*, Phys. Rev. D **74**, 094508 (2006).
[14] C. Aubin *et al.*, Phys. Rev. D **70**, 094505 (2004).
[15] M. Göckeler *et al.*, Phys. Lett. B **627**, 113 (2005).
[16] G. Martinelli *et al.*, Nucl. Phys. **B445**, 81 (1995); M. Göckeler *et al.*, Nucl. Phys. **B544**, 699 (1999).
[17] M. Göckeler *et al.*, Phys. Rev. Lett. **92**, 042002 (2004).
[18] M. Göckeler *et al.*, Nucl. Phys. **A755**, 537 (2005).
[19] Ph. Hägler *et al.*, Phys. Rev. D **68**, 034505 (2003).
[20] M. Diehl *et al.*, arXiv:hep-ph/0511032.
[21] D. Brömmel *et al.*, arXiv:hep-lat/0608021.
[22] M. Göckeler *et al.*, arXiv:hep-lat/0610118.
[23] A. Ali Khan *et al.*, Nucl. Phys. **B689**, 175 (2004).
[24] S. I. Ando, J. W. Chen, and C. W. Kao, arXiv:hep-ph/0602200; M. Diehl, A. Manashov, and A. Schäfer, arXiv:hep-ph/0608113.
[25] B. Pasquini, M. Pincetti, and S. Boffi, Phys. Rev. D **72**, 094029 (2005).
[26] M. Burkardt, arXiv:hep-ph/0611256.
[27] Ph. Hägler *et al.*, Phys. Rev. Lett. **93**, 112001 (2004).
[28] H. Avakian *et al.*, Jefferson Lab Research Proposal No. PR12-06-112.
[29] See baseline technical report, PANDA Collaboration, http://www.gsi.de/fair/reports/btr.html.